Available online at www.sciencedirect.com
ScienceDirect
Journal of Sound and Vibration 307 (2007) 379–385
JOURNAL OF SOUND AND VIBRATION
www.elsevier.com/locate/jsvi

Short Communication

A preliminary experimental study on virtual sound barrier system

Haishan Zou*, Xiaojun Qiu, Jing Lu, Feng Niu

Key Laboratory of Modern Acoustics and Institute of Acoustics, Nanjing University, Nanjing 210093, People's Republic of China

Received 19 September 2006; received in revised form 15 May 2007; accepted 23 June 2007

Abstract

Virtual sound barrier (VSB) is an array of loudspeakers and microphones forming an acoustic barrier, which creates a quiet zone without blocking air and light. A 16-channel cylindrical VSB system has been developed and its feasibility is verified by both numerical simulations and experiments. Experimental results in a normal room show that it can create a quiet zone larger than the size of a human head in the low-middle frequency, with a total sound pressure level reduction of more than 10 dB in the quiet zone. The control performance of the system with respect to the frequency, the distribution of the error sensors and the control sources are discussed.

1. Introduction

Local control and global control are two strategies of active control of sound [1]. Global control is most effective in an enclosure with a few acoustical modes, which corresponds to low frequency or a very small enclosure [2]. In an enclosure with high modal density or in free sound field, global control can be achieved only when the distance between the primary source and the control sources is less than a half wavelength [3,4]. In some cases, it is hard to put the control sources near the primary source. Thus, the local control strategy of which the objective is to create quiet zones in a desired area instead of the global control should be applied.

To create a quiet zone, a control source is used to cancel the pressure at a closely spaced error sensor. In a diffuse sound field, the shape of the quiet zone (the 10 dB reduction area) is a sphere centered on the error sensor with a diameter not greater than one-tenth of a wavelength [5,6]. A typical application is the active headrest that uses two loudspeakers to reduce the sound pressure around the ear positions (two separate points) of a listener. Nevertheless, in a free sound field, an array of control sources and error sensors forming an active noise barrier (ANB) is usually used to block the noise in a certain direction, producing a quiet zone behind the barrier. Early work combined the active control techniques with the passive barrier, where control sources were used to control the diffraction sound along the edge of the passive barrier [7,8], and recent work shows that the ANB system (without passive barrier) can be used independently to control low-frequency noise propagation [9–11].

*Corresponding author. Tel.: +86 25 8359 4505; fax: +86 25 83592919.
E-mail address: hszou@nju.edu.cn (H. Zou).

0022-460X/$ - see front matter © 2007 Elsevier Ltd. All rights reserved.
doi:10.1016/j.jsv.2007.06.042

ANB system is only able to control the noise coming from a certain direction, so it is usually used as a traffic barrier along roads. The active headrest can work in general condition but the size of the quiet zone created is so small that the movement of the human head is limited. The virtual sound barrier (VSB) system reported in this communication is an array of loudspeakers and microphones spaced in three-dimensional close structure to create a quiet zone within the space surrounded by the error sensors. The system can work in the environment in which the noise comes from many different directions, for example in a diffuse sound field. Compared to the active headrest, it uses multiple channels to enlarge the active range of the human head.

A numerical model of the VSB system was proposed and its feasibility was verified by the simulation results [12]. An experiment VSB system has been developed and is reported in this communication. Experiment results in a normal room show that it can create a quiet zone larger than the size of a human head in the low-middle frequency range, with a total sound pressure level reduction of more than 10 dB in the quiet zone. Finally, the effective frequency range, the variation of performance with respect to the distribution of the error sensors and the control sources are investigated as well.

2. Theoretical basis

The sound fields are assumed to be harmonic and an optimal control is derived through numerical computations in frequency domains. The primary noise field at point $\mathbf{r}$ is assumed to consist of a number of plane waves with random phases from many different directions as

$$p_p(\mathbf{r}) = \frac{1}{\sqrt{N_p}} \sum_{i=1}^{N_p} P_{pi}(\mathbf{r}) = \frac{1}{\sqrt{N_p}} \sum_{i=1}^{N_p} P_{Ai} \mathrm{e}^{-\mathrm{j}k(\varphi_{0i} + n_i \cdot r)}, \tag{1}$$

where $k = 2\pi f / c_0$ is the wavenumber, c_0 the speed of sound in the air and f the frequency. The ith plane wave with amplitude P_{Ai} comes from a random direction $\mathbf{n}_i$ with a randomly related phase φ_{0i}. The amplitude P_{Ai} and the phase φ_{0i} are taken from a uniform distribution of $(0, 1)$ and $(-\pi, \pi)$, respectively. $\mathbf{n}_i$ is a random unit vector. When N_p is sufficiently large (100 is used in the simulation), the primary sound field given above can be used to simulate a diffuse sound field [1]. The primary field calculated using the method outlined above is only one sample of an infinite ensemble of the possible diffuse pressure fields. The estimate of the mean square pressure, which characterises such an ensemble of diffuse sound fields, is calculated from 20 samples of diffuse sound fields, each calculated from Eq. (1).

Control sources can be treated as monopoles in low frequency. Only the direct sound of the control sources is taken into account for simplicity. The control sound field generated by N_c control sources can be expressed as

$$p_c(\mathbf{r}) = \sum_{m=1}^{N_c} \frac{j\omega\rho_0 q_m}{4\pi \left| \mathbf{r} - \mathbf{r}_m^c \right|} \mathrm{e}^{-\mathrm{j}k|r - r_m^c|} = \sum_{m=1}^{N_c} Z_m(\mathbf{r}) q_m = \mathbf{Z}_c(\mathbf{r}) \mathbf{q}_c, \tag{2}$$

where ρ_0 is the air density. $\mathbf{Z}_c(\mathbf{r}) = [Z_1(\mathbf{r}), Z_2(\mathbf{r}) \cdots Z_{Nc}(\mathbf{r})]$ is the row vector of acoustic transfer impedances from the control sources to the observation position. $\mathbf{q}_c = [q_1, q_2 \cdots q_{Nc}]^{\mathrm{T}}$ is the vector of source strengths of control sources. The total sound field is given by

$$p_t(\mathbf{r}) = p_p(\mathbf{r}) + p_c(\mathbf{r}) = p_p(\mathbf{r}) + \mathbf{Z}_c(\mathbf{r}) \mathbf{q}_c. \tag{3}$$

The sum of the squared sound pressures at error sensor positions is selected as the cost function:

$$J_p = \sum_{n=1}^{N_e} \left| p_t(\mathbf{r}_n^e) \right|^2 + \beta \mathbf{q}_c^H \mathbf{q}_c, \tag{4}$$

where N_e is the number of error sensors located at $\{\mathbf{r}_n^e, n = 1,2,\ldots N_e\}$. β is a positive real number, which is used to determine the weighting for the control effort term. The effect of the control effort term is to maintain the stable and consistence performance of the system under various conditions. The optimal strengths of the control sources is adjusted to

$$\mathbf{q}_c = -(\mathbf{Z}_{ce}^H \mathbf{Z}_{ce} + \beta \mathbf{I})^{-1} \mathbf{Z}_{ce}^H \mathbf{p}_{pe}, \tag{5}$$

where $\mathbf{Z}_{ce} = [\mathbf{Z}_c(\mathbf{r}_1^e), \mathbf{Z}_c(\mathbf{r}_2^e) \cdots \mathbf{Z}_c(\mathbf{r}_N^e)]^{\mathrm{T}}$ is the $N_e \times N_c$ matrix of transfer impedances from control sources to the error sensors, and $\mathbf{p}_{pe} = [p_p(\mathbf{r}_1^e), p_p(\mathbf{r}_2^e) \cdots p_p(\mathbf{r}_N^e)]^{\mathrm{T}}$ is the vector of sound pressures at the error sensor positions due to the primary noise field. A rule of thumb is to set β between 1/1000 and 1/5000 of the largest eigenvalue of the matrix $\mathbf{Z}_{ce}^H \mathbf{Z}_{ce}$. For such values of β the solution tends to be well-behaved, judged by subjective standards [13]. After obtaining the optimal control source strength, it is substituted back to Eq. (3) to calculate the total sound pressure amplitude after control.

The performance of the VSB system is defined as the ratio of the sum of the squared sound pressure inside the volume surrounded by error sensors without and with control as

$$NR = 10 \log 10 \left[\sum_{i=1}^{N_v} |p_p(\mathbf{r}_i)|^2 / \sum_{i=1}^{N_v} |p_t(\mathbf{r}_i)|^2 \right], \tag{6}$$

where N_v is the number of evaluation points, which is chosen to ensure at least six evaluation points per wavelength.

3. Simulations and experiments

3.1. System configuration

Fig. 1 shows the setup of the VSB system of 16 channels that is investigated. The 16 error sensors are spaced on two horizontal planes separated by h_e, and the eight error sensors in each plane are evenly spaced on a circle of radius $a_e = h_e$. The control sources are located similarly surrounding the error sensors with the two horizontal planes separated by h_c and the circle of radius $a_c = h_c$.

Experiments were carried out in a normal room of about $4 \times 5 \times 4\,\mathrm{m}^3$. The shape of the room is not regular, and there are three narrow corridors connected to other rooms. Furthermore, there are aluminous doors and thick iron doors distributed around the walls, which make the reflection quite complicated. The primary noise sources were three loudspeakers located in three different directions and at the height of 1.2, 3.0 and 0.5 m, respectively. Their inputs were from a same amplified pure-tone signal. With the reflections of all the surfaces of the room, the sound field in the room is closed to the supposed primary sound field mentioned above. The VSB system was placed in the center of the room with the central horizon plane 0.8 m above the floor. A total of 16 speakers and 16 microphones were used as control sources and error sensors, respectively. A 16-channel ANC controller using the filter-x LMS algorithm was applied. The pure-tone signal generated by the signal generator was also fed into the controller as the reference signal. The distance between each primary source and the center of the system was about 4 m. Additional measuring microphones were used to measure the sound pressure in the target region and the intervals of measurement grid were less than 1/6 wavelength of the noise signal.

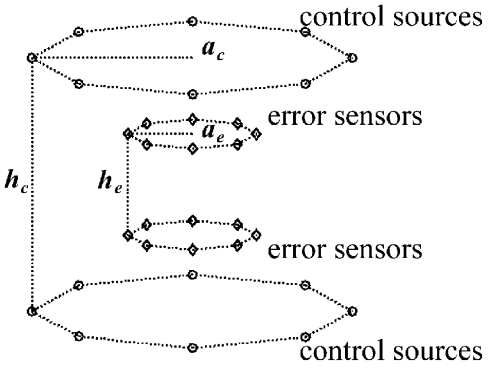

Fig. 1. Setup of the VSB system of 16 channels.

Fig. 2 shows the location of the experimental setup in the room. It is a schematic platform so that the control sources, the error sensors and the measurement sensors are superposed in vertical directions. Fig. 3 is a photo of the experimental setup.

3.2. The control performance of the VSB system

While many factors affect the performance of the VSB system, only the frequency, the arrangement of the control sources and the errors sensors are investigated below. The performance with respect to the frequency is

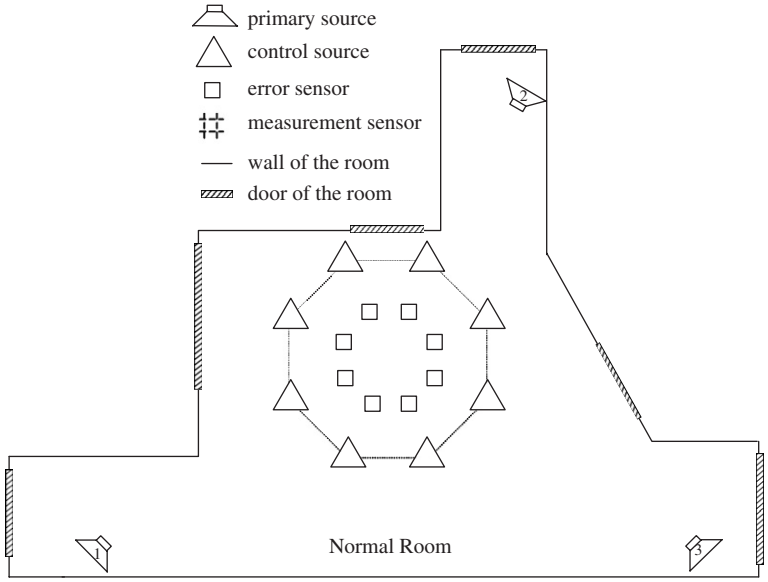

Fig. 2. Experimental setup.

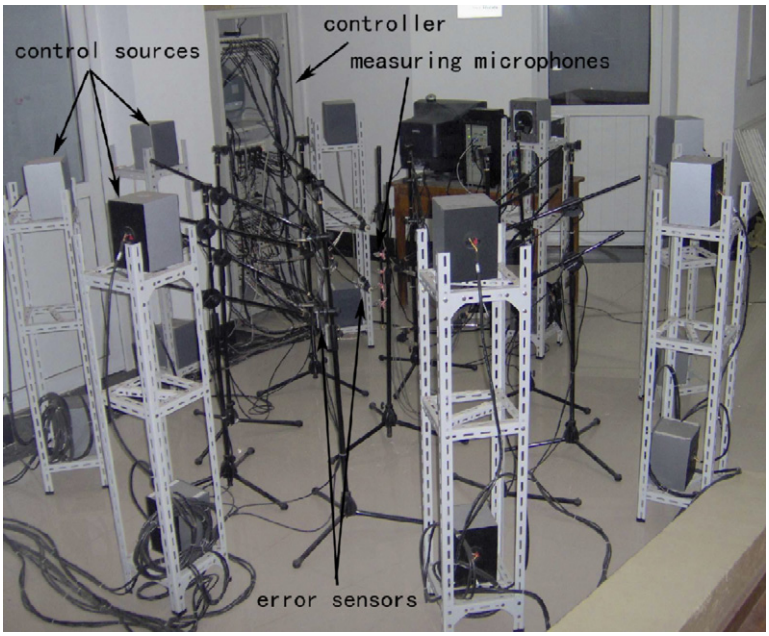

Fig. 3. Photo of the experimental setup.

investigated firstly, when the arrangement of the control sources and the error sensors is fixed. For the easy movement of the listener's head, a_e is set to no less than 0.2 m. Eleven typical sinusoidal noise signals are controlled by the system in the experiment with $a_c = 1.22$ m, $a_e = 0.2$ m, and the frequencies are between 200 and 700 Hz with 50 Hz interval. The control performance is shown in Fig. 4, in which it can be seen that the noise reduction level within the quiet zone decreases with the increase of the noise frequency in both the experimental and simulation results. The noise reduction of 200 and 250 Hz are less than expected in the experimental curve because the practical controller can only obtain about 30 dB in practice.

The feasibility of the VSB system to acquire a quiet zone larger than a human head is verified in Fig. 4. As long as the noise frequency is below 550 Hz, an effective quiet zone can be achieved. The diameter of the volume surrounded by the error sensors is 0.66λ (about 0.4 m for 550 Hz). Compared with the quiet zone size of the active headrest system, the enlargement of the quiet zone is at the cost of the multi-channel of the VSB system.

The control performance of the VSB system is affected by the distribution of the error sensors and the control sources as well. The control performance with respect to a_e in 250 Hz is shown in Fig. 5, with $a_c = 0.9\lambda = 1.22$ m. The parameter a_e is equal to $i \times 0.07\lambda$ ($i = 1, \ldots, 5$) in the experiment. Both the simulation and the experiment demonstrate that the control performance deteriorates as a_e is increased. a_e must be less than 0.34λ (about 0.44 m for 250 Hz) to obtain an effective quiet zone. The theoretical background of VSB can be traced back to Huygens' principle and the Kirchhoff–Helmholtz integral equation [12], the sound field within the volume surrounded by the error sensors is determined by the sound field of the cylindrical surface surrounding the volume. When a_e is increased, i.e. the interval of the error sensors becomes larger, the distribution of the sound pressure on the surface will not be reduced uniformly and the reduction of the sound pressure in the volume will be decreased. The reason that the sound pressure reduction in the experiment is much less than that in the simulation result when a_e is equal to 0.07λ in Fig. 5 is also due to the restriction of the practical controller.

The control performance with respect to $a_c - a_e$ in 250 Hz is shown in Fig. 6, with $a_e = 0.28\lambda = 0.38$ m. The radius of the control sources are $a_c = \{0.48\ 0.55\ 0.63\ 0.73\ 0.9\}\lambda$ in the experiment. Fig. 6 indicates that when a_c is close to a_e, the control performance improves rapidly with an increase in a_c. When $a_c - a_e$ exceeds some certain value ($a_c - a_e < 0.3\lambda$ in the experiment and $a_c - a_e < 0.2\lambda$ in the simulation), the control performance fluctuates slightly. As shown in Fig. 1, the error sensor array and the control source array have the same geometrical configuration. When a_c is very close to a_e, the distance between an error sensor and the

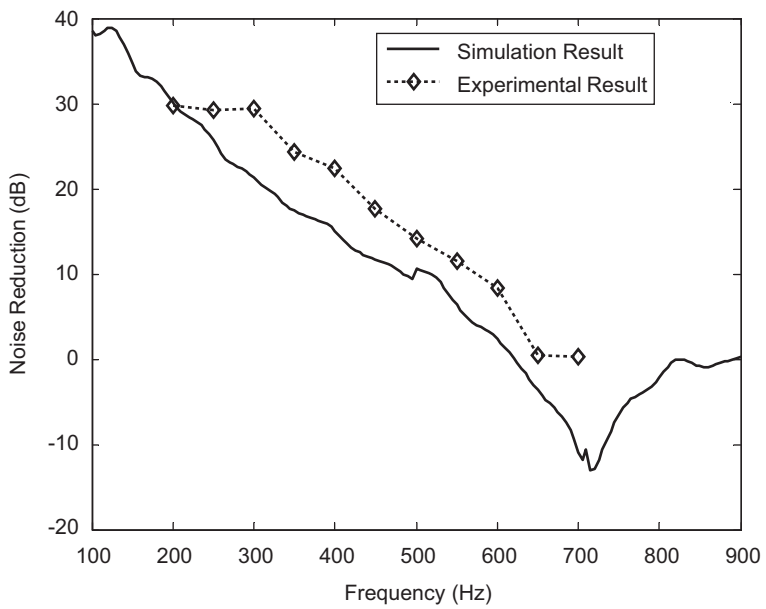

Fig. 4. Control performance with respect to the frequency of the noise signal, $a_c = 1.22$ m, $a_e = 0.2$ m.

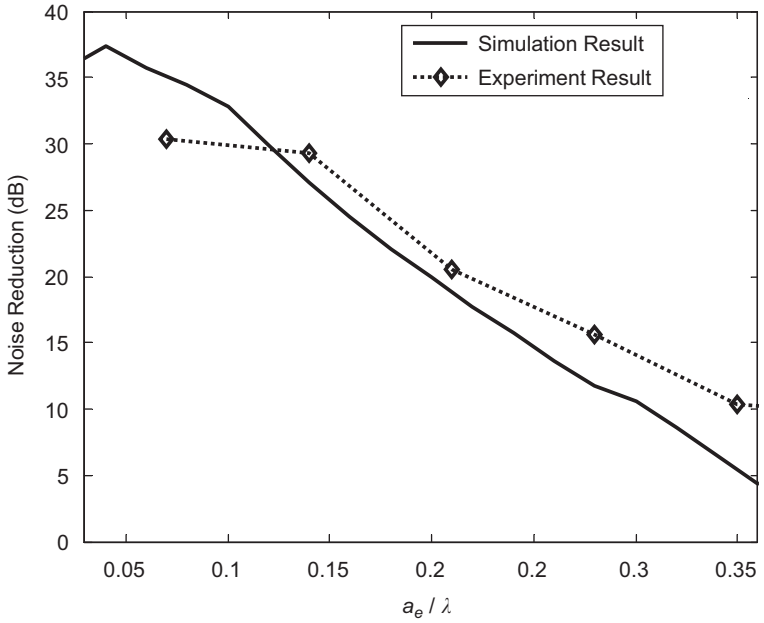

Fig. 5. Control performance with respect to a_e, $f = 250\,\text{Hz}$, $a_c = 1.22\,\text{m}$.

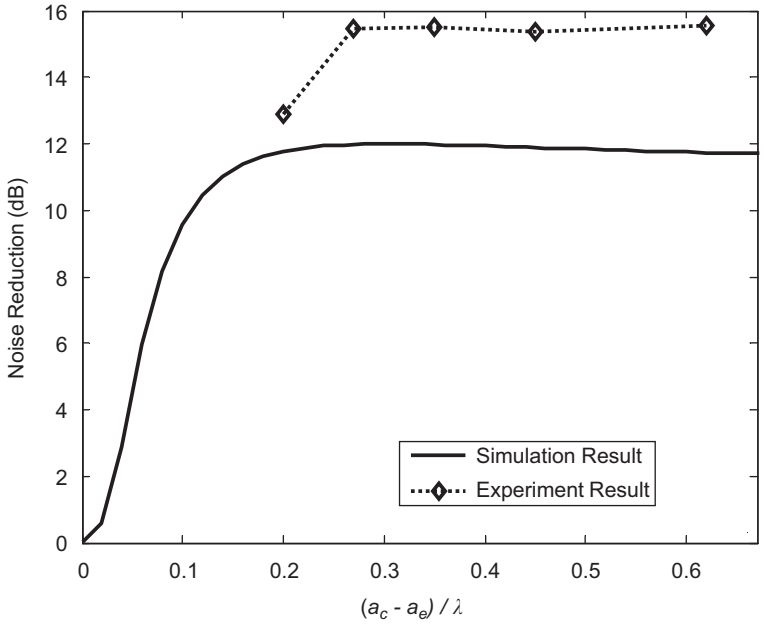

Fig. 6. Control performance with respect to $a_c - a_e$, $f = 250\,\text{Hz}$, $a_e = 0.38\,\text{m}$.

corresponding control source is much less than that between this error sensor and any other control source. This results in $Z_m(\mathbf{r}_m^e)$ being much larger than $Z_m(\mathbf{r}_n^e)$, $m \neq n$. Because the optimal strength q_m is dominated by the inverse of $Z_m(\mathbf{r}_m^e)$, only a very small value of q_m is required to control the corresponding error sensor at point $\mathbf{r}_m^e$. But with a very small value, q_m can only control a very small zone, so the sound pressure on the entire cylindrical surface will not be reduced uniformly and the control effect in the volume is weak. The optimal strengths increase with the increasing $a_c - a_e$, and this enlarges the 'covering zone' of the control sources. When $a_c - a_e$ exceeds a certain value, the control sources can affect the entire cylindrical surface and

the volume can be controlled effectively. After that, although the optimal strengths still become larger with an increase in $a_c - a_e$, the control performance fluctuates slightly. As a result, it is unnecessary to enlarge the size of the system any further.

There are differences between the experimental and simulation results shown in Figs. 4–6, which might be caused by the difference between the experimental configurations and the numerical model. For example, the numerical model of the primary sound field consists of many samples of diffuse sound fields calculated from Eq. (1), but the primary sound field in the experiment is just only one sample of the diffuse sound fields. Furthermore, only the direct sound of the control sources is taken into account in numerical simulations. Finally, attention should be paid to the fact that the distances from the primary sources and the control sources were larger than a half-wavelength of the noise signal in all experiments, so that the control mechanism of VSB is not the global control for minimizing the total power output of primary and control sources [3,4].

4. Conclusions

A 16-channel cylindrical VSB has been developed and its feasibility has been verified by both numerical simulations and experiments. In a normal room where the noise comes from many different directions, the upper limiting frequency can be up to 550 Hz, with the average reduction of more than 10 dB inside a cylindrical region with 0.2 m height and 0.2 m radius. The control performance of the system decreases with the increase of the noise frequency. Furthermore, the control performance of the system is affected by the distribution of the error sensors and the control sources. The intervals between the error sensors have an upper limitation and the distances between the control sources and the error sensors have a lower limitation. A number of practical problems need to be further studied in the future, such as the influence of a diffraction object like a human head, the broadband control and a more accurate model in time domain.

Acknowledgments

Project 10304008 and 10674068 is supported by NSFC.

References

[1] P.A. Nelson, S.J. Elliott, *Active Control of Sound*, Academic Press, London, 1992.
[2] A.J. Bullmore, P.A. Nelson, A.R.D. Curtis, S.J. Elliott, The active minimization of harmonic enclosed sound fields, part II: a computer simulation, *Journal of Sound and Vibration* 117 (1987) 15–33.
[3] P.A. Nelson, A.R.D. Curtis, S.J. Elliott, A.J. Bullmore, The active minimization of harmonic enclosed sound fields, part I: theory, *Journal of Sound and Vibration* 117 (1987) 1–13.
[4] P.A. Nelson, A.R.D. Curtis, S.J. Elliott, A.J. Bullmore, The minimum power output of free field point sources and the active control of sound, *Journal of Sound and Vibration* 116 (1987) 397–414.
[5] S.J. Elliot, P. Joseph, A.J. Bullmore, P.A. Nelson, Active cancellation at a point in a pure tone diffuse sound field, *Journal of Sound and Vibration* 120 (1988) 183–189.
[6] A. David, S.J. Elliot, Numerical studies of actively generated quiet zones, *Applied Acoustics* 41 (1994) 63–79.
[7] A. Omoto, K. Fujiwara, A study of an actively controlled noise barrier, *Journal of the Acoustical Society of America* 94 (1993) 2173–2180.
[8] A. Omoto, K. Takashima, K. Fujiwara, Active suppression of sound diffracted by a barrier: an outdoor experiment, *Journal of the Acoustical Society of America* 102 (1997) 1671–1679.
[9] H. Nagamatsu, S. Ise, K. ShiKano, Numerical study of active noise barrier based on the boundary surface control principle, *Proceedings of Active 99*, Fort Lauderdale, Florida, 1999, pp. 585–594.
[10] M. Hodgson, J. Guo, P. Germain, Active local control of propeller-aircraft run-up noise, *Journal of the Acoustical Society of America* 114 (2003) 3201–3210.
[11] J. Guo, J. Pan, Further investigation on actively created quiet zones by multiple control sources in free space, *Journal of the Acoustical Society of America* 102 (1997) 3050–3053.
[12] X. Qiu, N. Li, G. Chen, Feasibility study of developing practical virtual sound barrier system, *Proceedings of 12th International Congress on Sound and Vibration*, Lisbon, Portugal, 2005.
[13] O. Kirkeby, P.A. Nelson, F.O. Bustamante, H. Hamada, Local sound field reproduction using digital signal processing, *Journal of the Acoustical Society of America* 100 (1996) 1584–1593.